NADPH Oxidase-1 Plays a Crucial Role in Hyperoxia-induced Acute Lung Injury in Mice

Stéphanie Carnesecchi[1,2], Christine Deffert[1,2], Alessandra Pagano[1,2], Sarah Garrido-Urbani[2], Isabelle Métrailler-Ruchonnet[1,2], Michela Schäppi[1,2], Yves Donati[1,2], Michael A. Matthay[3], Karl-Heinz Krause[2,4], and Constance Barazzone Argiroffo[1,2]

[1]Department of Pediatrics and [2]Department of Pathology and Immunology, Medical School, University of Geneva, Geneva, Switzerland; [3]Department of Anesthesia, University of California, San Francisco, San Francisco, California; and [4]Department of Genetic and Laboratory Medicine, Geneva University Hospitals, Geneva, Switzerland

Rationale: Hyperoxia-induced acute lung injury has been used for many years as a model of oxidative stress mimicking clinical acute lung injury and the acute respiratory distress syndrome. Excess quantities of reactive oxygen species (ROS) are responsible for oxidative stress–induced lung injury. ROS are produced by mitochondrial chain transport, but also by NADPH oxidase (NOX) family members. Although NOX1 and NOX2 are expressed in the lungs, their precise function has not been determined until now.

Objectives: To determine whether NOX1 and NOX2 contribute *in vivo* to hyperoxia-induced acute lung injury.

Methods: Wild-type and NOX1- and NOX2-deficient mice, as well as primary lung epithelial and endothelial cells, were exposed to room air or 100% O_2 for 72 hours.

Measurements and Main Results: Lung injury was significantly prevented in NOX1-deficient mice, but not in NOX2-deficient mice. Hyperoxia-dependent ROS production was strongly reduced in lung sections, in isolated epithelial type II cells, and lung endothelial cells from NOX1-deficient mice. Concomitantly, lung cell death *in situ* and in primary cells was markedly decreased in NOX1-deficient mice. In wild-type mice, hyperoxia led to phosphorylation of c-Jun N-terminal kinase (JNK) and extracellular signal–regulated kinase (ERK), two mitogen-activated protein kinases involved in cell death signaling, and to caspase-3 activation. In NOX1-deficient mice, JNK phosphorylation was blunted, and ERK phosphorylation and caspase-3 activation were decreased.

Conclusions: NOX1 is an important contributor to ROS production and cell death of the alveolocapillary barrier during hyperoxia and is an upstream actor in oxidative stress–induced acute lung injury involving JNK and ERK pathways in mice.

Keywords: NADPH oxidase; reactive oxygen species; hyperoxia; apoptosis; mitogen-activated protein kinases

Respiratory distress syndrome (RDS) of premature babies is characterized by immature lung development and insufficient surfactant production by alveolar type II cells. During RDS treatment with mechanical ventilation and high oxygen concentration, the lungs are exposed to increased oxidative stress leading to pulmonary injury (1). The damage to both endothe-

---

AT A GLANCE COMMENTARY

Scientific Knowledge on the Subject

Oxidative stress is a major feature of acute lung injury and the acute respiratory distress syndrome (ARDS) and may be responsible for pulmonary cell damage.

What This Study Adds to the Field

Targeting the NADPH oxidase NOX1 during hyperoxia-induced lung injury in mice inhibits oxidative-induced cell death pathway and lung damage, providing a new therapeutic approach in the treatment of acute lung injury.

lial and epithelial cells leads to the loss of alveolocapillary barrier integrity, resulting in interstitial edema and gas exchange impairment. We and others have previously shown that reactive oxygen species (ROS) are able to induce a cell death response with features of both apoptosis and necrosis during oxygen exposure (2, 3). The mechanisms of cell death are not completely defined in hyperoxia-mediated lung epithelial and endothelial cell death, but involve the activation of mitogen-activated protein kinase (MAPK) (4) and the caspase cascade (5). Inhibition of the c-Jun N-terminal kinase (JNK) or extracellular signal–regulated kinase (ERK) pathway, using dominant negative constructs or chemical inhibitors, prevents cell death in an epithelial cell line (MLE-12) and in human pulmonary artery endothelial cells during hyperoxia (6–9).

During supplemental oxygen therapy, ROS can be generated by a variety of enzymes such as mitochondrial chain transport and NADPH oxidase enzymes (10, 11). The well-known phagocyte NADPH oxidase complex includes a catalytic subunit, NOX2/gp91[phox], which is associated with regulatory subunits (11). This complex is required for NOX activation and generation of superoxide (11, 12). The NOX2 complex plays an essential role in nonspecific host defense against pathogens (13). Several additional homologs of NOX2 have been identified: NOX1–NOX5, dual oxidase-1 (DUOX1), and DUOX2. Despite their similar structure and enzymatic function, NOX enzymes differ in their mechanism of activation. The NOX isoforms are expressed in several tissues and cell types, where they serve various physiological functions, including posttranslational modifications of proteins and cellular signal transduction (12, 14, 15). NOX enzymes are also involved in a variety of pathologies, including amyotrophic lateral sclerosis, hypertension, and lung emphysema (16–19).

A study demonstrated that both NOX1 and NOX2 are expressed in mouse lung, and NOX1 has been detected in a human alveolar epithelial cell line (A549) and in endothelial

cells (20, 21). However, until now, no precise function of NOX1 and NOX2 in the lungs has been determined. *In vitro* studies demonstrated that diphenylenethidium (DPI), a wide inhibitor of NADPH oxidases, was effective in reducing hyperoxia-induced ROS generation and cell death in MLE-12 cells and in pulmonary endothelial cells (6, 9, 22). Using NOX1- and NOX2-deficient mice, we determined their specific contribution in hyperoxia-induced acute lung injury.

This study demonstrates for the first time that NOX1, but not NOX2, is an important mediator of acute lung injury mediated by oxidative stress, particularly in alveolar cells. NOX1-generated ROS are largely responsible for alveolar cell death and subsequent lung injury through JNK and ERK pathways

during hyperoxia in mice. Some of these data have been reported in the form of an abstract (23).

METHODS

See the online supplement for additional details on reagents and methods.

Animals

NOX1-deficient mice, NOX2 (gp91^{phox})-deficient mice, and wild-type (WT) mice were inbred on the C57BL/6J background (17, 24). Animals were kept under specific pathogen–free conditions. The animal procedure was performed in accordance with the Institutional Ethics
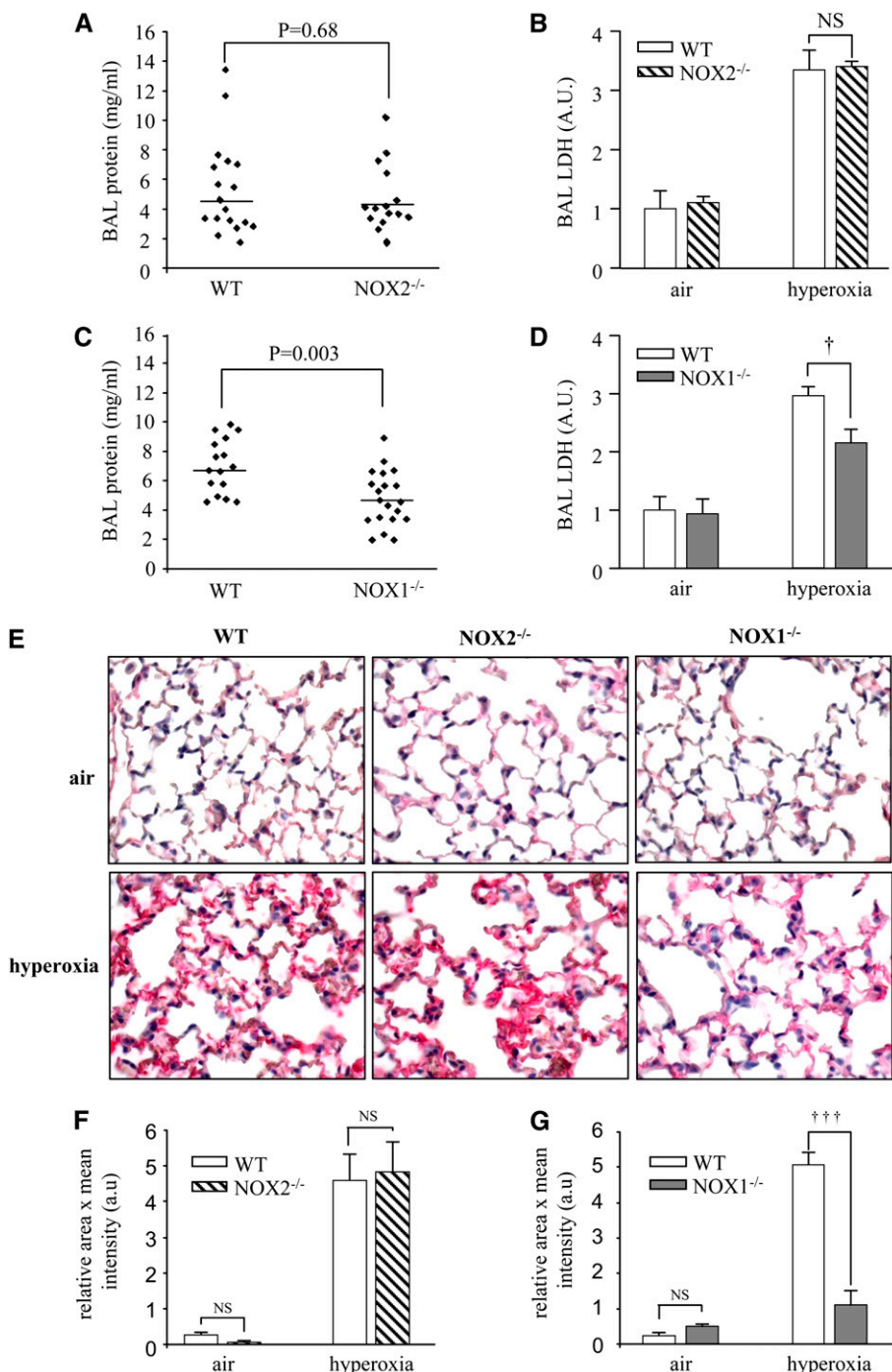
Figure 1. Lung injury is decreased in NADPH oxidase-1 (NOX1)-deficient but not in NADPH oxidase-2 (NOX2)-deficient mice. NOX1$^{-/-}$, NOX2$^{-/-}$, and wild-type (WT) mice were exposed to 100% hyperoxia for 72 hours. (*A*) Bronchoalveolar lavage (BAL) protein content (n ≥ 15 in each group; $P = 0.68$ compared with WT) and (*B*) BAL lactate dehydrogenase (LDH) content in NOX2$^{-/-}$ mice (n = 5 or 6 for each group; P = not significant [NS], NOX2$^{-/-}$ mice vs. WT in hyperoxia). (*C*) BAL protein content (n > 15 for each group; $P = 0.003$ compared with WT mice) and (*D*) BAL LDH content in NOX1$^{-/-}$ mice (n = 10 in each group; $^{†}P < 0.05$, NOX1$^{-/-}$ mice vs. WT in hyperoxia). *Columns* and *error bars* represent the mean ± SEM. (*E*) Immunochemical detection of fibrin in paraffin-embedded lung sections. Lung sections were stained with a polyclonal anti-fibrin antibody (*red*) and visualized by optical microscopy. Original magnification, ×40. (*F*) Quantification of fibrin deposition in NOX2$^{-/-}$ mice and their WT control. Values represent the mean of the relative area × mean of intensity ± SEM of 10 different fields (n = 3 mice in each group); P = NS, NOX2$^{-/-}$ mice versus WT in hyperoxia. (*G*) Quantification of fibrin deposition in NOX1$^{-/-}$ mice and their WT control; $^{†††}P < 0.001$, NOX1$^{-/-}$ mice versus WT in hyperoxia.

Committee on Animal Care (Geneva, Switzerland) and the Cantonal Veterinary Office.

Hyperoxia Exposure

Eight- to 10-week-old female mice (deficient and WT) were exposed to room air or 100% O_2 for 72 hours. Bronchoalveolar lavage (BAL) was performed as described (25). The total cell count was determined with a cell counter and protein concentration was measured. BAL fluid cell distribution was quantified in Cytospin preparations (Perbio Science, Lausanne, Switzerland) after staining with Diff-Quik dye (Dade Behring, Paris, France).

Lung Histology and Immunohistochemistry

Paraffin-embedded sections of lung fixed in 4% paraformaldehyde were stained with hematoxylin–eosin or with anti-fibrin polyclonal antibody followed by EnVision G|2 System/AP (Dako, Glostrup, Denmark), or with an anti–cleaved caspase-3 polyclonal antibody followed by Texas red–conjugated secondary antibody. Double immunostaining was performed with anti-pJNK (phosphorylated JNK) or anti-pERK (phosphorylated ERK) monoclonal antibody combined with anti– SP-C (Chemicon, Zug, Switzerland) or anti–von Willebrand factor (VWF) followed by fluorescein isothiocyanate–conjugated secondary antibody before counterstaining with 4′,6-diamidino-2-phenylindole (DAPI). Slides were mounted with Fluor Save (Calbiochem, Darmstadt, Germany) and analyzed by confocal microscopy.

Alveolar Macrophage, Epithelial Type II Cell, and Endothelial Cell Isolation

Alveolar macrophages were isolated from the BAL fluid of adult mice, and alveolar epithelial type II cells (type II AECs) and endothelial cells (MLECs) were isolated from adult mouse (8- to 14-wk-old) lungs as described with minor modifications (26–28). Hyperoxic conditions (24–72 h) were achieved by placing type II AECs and MLECs in a sealed glass chamber filled with 95% O_2−5% CO_2 at 37°C.

Real-time Polymerase Chain Reaction

RNA was extracted with a total RNA isolation NucleoSpin RNA II kit (Macherey-Nagel, Düren, Germany) and reverse transcribed with SuperScript reverse transcriptase (SuperScript choice system; Invitrogen, Carlsbad, CA). We used the primers for NOX1, NOX2, and NOX4 and the reference genes encoding EEF1A1 (eukaryotic elongation factor-1A1) and HPRT (hypoxanthine–guanine phosphoribosyltransferase). For polymerase chain reaction primer sequences and details, *see* the online supplement.

Detection of Superoxide

Frozen lung tissues were cryosectioned (20 μm) and collected onto SuperFrost Plus slides (Perbio Science). To detect the various cell types that generated ROS, lung sections from all mouse strains were double immunostained with dihydroethidium (DHE) and anti–SP-C or with DHE and anti-VWF. Images were captured with an inverted microscope and analyzed with Metafluor imaging software (Molecular Devices, Basel, Switzerland). Quantification was performed by measuring the fluorescence intensity of all cells counted in the lung sections and of isolated type II and endothelial cells (>50 for each mouse) from three different mice.

Western Blot Analysis

Total lung protein extracts were performed as previously described (29). Total protein extracts were loaded and nitrocellulose membranes were blocked overnight in Tris-buffered saline–Tween buffer, 5% milk, followed by hybridization with anti-pJNK, anti-JNK, anti-pERK, anti-ERK, anti-actin, anti–cleaved caspase-3, or anti-poly(ADP-ribose) polymerase (PARP)-1 in the same buffer. The proteins were detected with enhanced chemiluminescence (ECL) reagents (Interchim, Montluçon, France). Densitometric evaluation was performed with Quantity One software (Bio-Rad, Reinach, Switzerland).

Measures of Cell Death

Lactate dehydrogenase was measured in BAL supernatant as described (30). For sections of fixed lung, terminal deoxynucleotidyl-transferase–mediated dUTP nick end labeling (TUNEL) was performed with an *in situ* apoptosis detection kit according to the protocol of the manufacturer (Chemicon, Temecula, CA); and for primary cells, TUNEL was performed as described by the manufacturer (Roche, Indianapolis, IN). Slides were mounted with polyvinyl alcohol (Mowiol) and analyzed by confocal microscopy (LSM 510 Meta; Zeiss, Oberkochen, Germany). Quantification of positive staining was performed with Metamorph analysis software (Molecular Devices) (20 images per mouse, 3 mice per group, and 3 independent experiments).

Statistical Analysis

For all parameters measured, the values for all samples under different experimental conditions were averaged and the SEM of the mean was calculated. The significance of differences between the values of the groups was determined by two-way analysis of variance with multiple comparisons followed by unpaired t test. The Wilcoxon rank sum test for unpaired data was also used. Significance levels were set at $P < 0.05$.

RESULTS

NOX1, But Not NOX2, Participates in Hyperoxia-induced Lung Injury

To address the role of NOX1 and NOX2 in hyperoxia-induced lung injury, we exposed NOX1- and NOX2-deficient mice, as well as WT mice, to 100% oxygen. In accordance with previous studies from our laboratory and others, WT mice exhibited features of severe lung damage after 72 hours of oxygen exposure. The extent of lung injury was not significantly different in NOX2-deficient mice compared with WT mice as measured by BAL protein content reflecting vascular leakage (Figure 1A); BAL lactate dehydrogenase release, an indicator of tissue injury (Figure 1B); and fibrin deposition in the alveolar spaces (Figures 1E−1G). In contrast, the absence of NOX1 significantly reduced hyperoxia-induced lung injury compared with WT mice (Figures 1C−1E and 1G). Most of the *in vivo*

TABLE 1. EFFECT OF NADPH OXIDASE-1 AND NADPH OXIDASE-2 DEFICIENCY ON INFLAMMATORY CELL RESPONSE DURING HYPEROXIA

| | Cell Number ($\times 10^4$) | | |
	Air	Hyperoxia	P Values
WT	6.77 ± 0.85	17.14 ± 2.10*	NS
NOX1$^{-/-}$	7.97 ± 0.71	16.81 ± 1.66*	NS
NOX2$^{-/-}$	6.78 ± 1.09	19.63 ± 3.51*	NS
Macrophages			
WT	6.23 ± 0.67	15.30 ± 1.83*	NS
NOX1$^{-/-}$	7.17 ± 0.65	11.81 ± 1.14*	NS
NOX2$^{-/-}$	5.47 ± 0.73	11.61 ± 1.09*	NS
Lymphocytes			
WT	0.59 ± 0.12	1.56 ± 0.25*	NS
NOX1$^{-/-}$	0.74 ± 0.09	1.51 ± 0.21*	NS
NOX2$^{-/-}$	0.47 ± 0.06	2.76 ± 1.09†	NS
Neutrophils			
WT	0.05 ± 0.01	0.76 ± 0.22*	†
NOX1$^{-/-}$	0.06 ± 0.01	3.47 ± 0.77*	‡
NOX2$^{-/-}$	0.23 ± 0.06	4.53 ± 0.62*	NS

Definition of abbreviations: NOX1 = NADPH oxidase-1; NOX2 = NADPH oxidase-2; NS = not significant; WT = wild type.

NOX1$^{-/-}$, NOX2$^{-/-}$, and WT mice were exposed to air or to hyperoxia for 72 hours. Cells recovered from bronchoalveolar lavage were counted and Cytospin preparations on microscope slides were made and stained for cellular differentials. Results represent the mean value ± SEM for each group (n = 10 animals per group).

* $P < 0.001$, hyperoxia versus air.

† $P < 0.05$, NOX1$^{-/-}$ mice versus WT mice in hyperoxia.

‡ $P < 0.001$, NOX2$^{-/-}$ mice versus WT mice in hyperoxia.
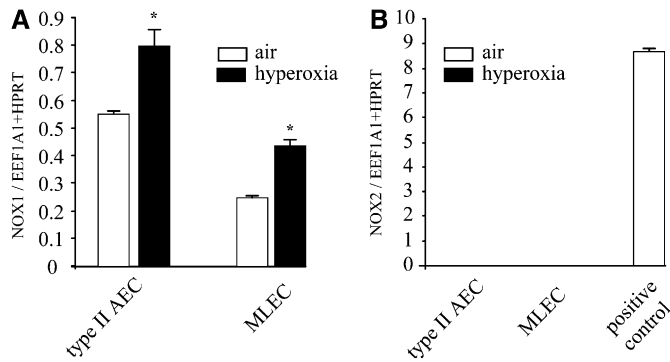
Figure 2. Hyperoxia up-regulates NADPH oxidase-1 (NOX1) mRNA expression in type II alveolar epithelial cells (AECs) and in mouse lung endothelial cells (MLECs). Expression of (*A*) NOX1 mRNA and (*B*) NADPH oxidase-2 (NOX2) mRNA in primary type II AECs and MLECs was measured by real-time polymerase chain reaction before and after 72 hours of hyperoxia (n = 3). *P < 0.05 in type II AECs and MLECs exposed to air (*open columns*) versus hyperoxia (*solid columns*). Note that primary alveolar macrophages were used as positive control for the detection of NOX2 mRNA expression. EEF1A1 = eukaryotic elongation factor-1A1; HPRT = hypoxanthine–guanine phosphoribosyltransferase.

experiments with NOX1- and NOX2-deficient mice were performed independently, each of them with their respective WT control. Under normal conditions, lungs of NOX1- and NOX2-deficient mice displayed no morphological abnormalities and were similar to those of WT mice (data not shown).

We then evaluated hyperoxia-induced lung inflammatory responses in NOX1- and NOX2-deficient mice. Hyperoxia caused a significant increase in BAL total cell count (macrophages, lymphocytes, and neutrophils) that was similar in the three mouse strains (Table 1). BAL neutrophil counts of NOX1- and NOX2-deficient mice were higher compared with those from WT mice in hyperoxia, but the neutrophil count was similar in air-breathing animals (Table 1). These results indicate that NOX1, but not NOX2, participates in oxidative stress–induced acute lung injury independently of the acute lung inflammatory response.

NOX1 Expression Is Increased in Primary Type II Alveolar Epithelial Cells and Lung Endothelial Cells in Hyperoxia

To determine whether NOX1 and NOX2 are regulated by hyperoxia in type II AECs and in MLECs, we measured NOX1 and NOX2 expression. At baseline, NOX1 mRNA was expressed in type II AECs and MLECs (Figure 2A), in contrast to NOX2 mRNA, which was undetectable compared with the positive control. As positive control, we used alveolar macrophages in which NOX2 is strongly expressed, as expected (Figure 2B). After hyperoxia, NOX1 mRNA expression was increased in both type II AECs and MLECs whereas NOX2 was still undetectable in these primary cells (Figures 2A and 2B).

NOX1 Deficiency Markedly Reduces Hyperoxia-induced ROS Production in Lungs and in Primary Pulmonary Cells

To determine the contribution of NOX1 in hyperoxia-induced superoxide formation, we measured ROS production in the lungs
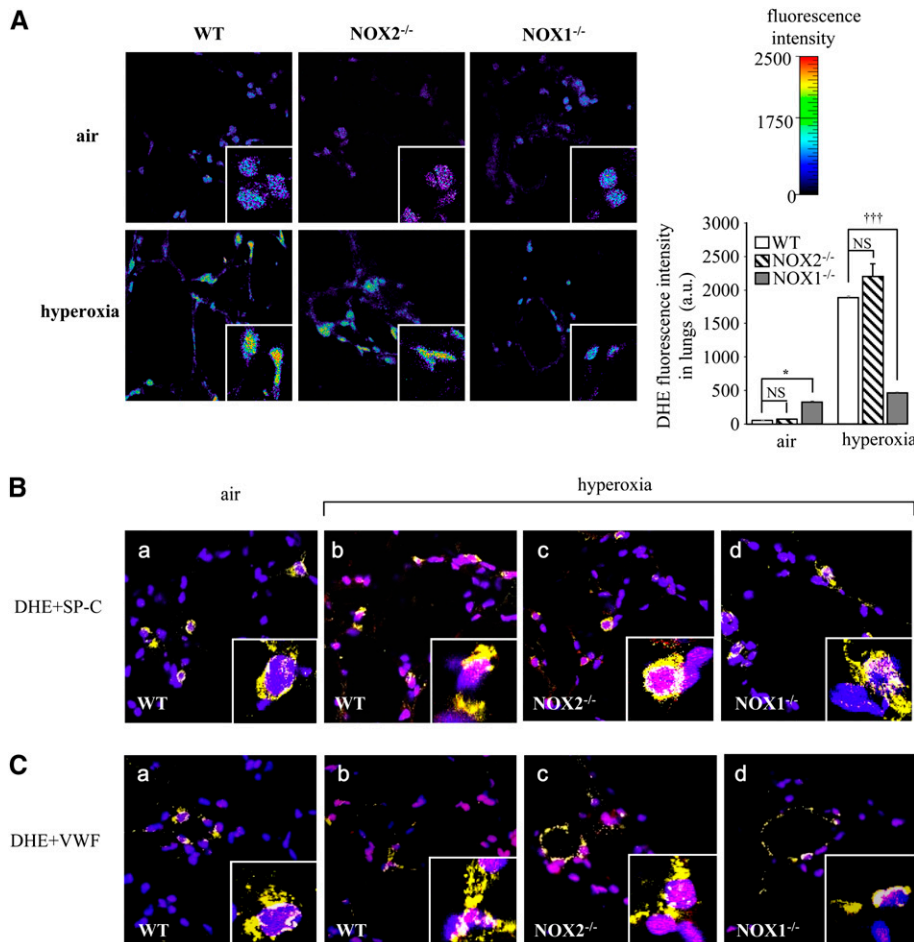
Figure 3. Absence of NADPH oxidase-1 (NOX1) decreased reactive oxygen species generation induced by hyperoxia in lungs. (*A*) Representative fluorescence images of dihydroethidium (DHE)-loaded lung sections. Frozen lung sections (20 μm) were prepared from NOX1$^{-/-}$, NOX2$^{-/-}$, and wild-type (WT) mice after exposure to air or hyperoxia for 72 hours. Lung sections were loaded with DHE (10 μM) and visualized by confocal microscopy (*pseudocolor*). Original magnification, ×63. DHE fluorescence intensity was quantified in whole lung sections (n = 3; *P < 0.05, NOX1$^{-/-}$ vs. WT mice, and P= NS, NOX2$^{-/-}$ vs. WT mice in air; †††P < 0.001, NOX1$^{-/-}$ vs. WT; and P = NS, NOX2$^{-/-}$ vs. WT mice in hyperoxia). (*B*) Representative merged images of lung sections stained with DHE (*pink*), 4′,6-diamidino-2-phenylindole (*blue*), and marker for type II epithelial cells (prosurfactant protein-C [SP-C]: *yellow*, panels a–d), or (*C*) marker for endothelial cells (von Willebrand factor [VWF]: *yellow*, panels a–d). DHE-positive nuclei appear *pink* and staining for both type II epithelial and endothelial markers appears *yellow*. Note that some cells were positive for DHE and cell-specific marker. Original magnification, ×63. NS = not significant.

of WT and NOX1-deficient mice. Mice were exposed to air or hyperoxia for 72 hours and frozen lungs were cryosectioned. Lung sections were stained with DHE for ROS detection. ROS were markedly increased in the lungs of hyperoxia-exposed WT mice compared with air-exposed WT mice. This hyperoxia-induced increase in ROS was significantly attenuated in NOX1-deficient mice but not in NOX2-deficient mice (Figure 3A).

To detect the various cell types generating ROS, we stained lung sections from WT and NOX2- and NOX1-deficient mice with DHE and an anti–SP-C antibody, or with DHE and an anti-VWF antibody. In wild-type mice, type II epithelial and endothelial cells were positive for DHE staining during hyperoxia in comparison with air-exposed WT mice (respectively: Figure 3B, panels a and b and Figure 3C, panels a and b). Hyperoxia-induced ROS in epithelial type II and endothelial cells were markedly decreased in NOX1-deficient mice, but were not modified in NOX2-deficient mice compared with WT mice (respectively: Figure 3B, panels c and d, and Figure 3C, panels c and d).

Similar results were found for isolated type II AECs (Figures 4A and 4C) and primary MLECs (Figures 4B and 4D) derived from WT and NOX1-deficient mice exposed to hyperoxia. In contrast, primary type II AECs and MLECs isolated from NOX2-deficient mice produced an equal amount of ROS compared with cells isolated from WT mice during hyperoxia stimulation (Figures 4A–4D).

Interestingly, under normoxic conditions, lungs of NOX1-deficient mice exhibited a small, but significant increase in ROS generation as compared with WT mice, possibly because of a compensatory effect of ROS produced by other NOX enzymes or NOX-independent enzymes (Figure 3A; and see Figure E1 in the online supplement). Indeed, we analyzed the expression of NOX enzymes (NOX1, NOX2, and NOX4) in

deficient mice and we did not find any up-regulation (Figure E1). This increase was not found in primary type II AECs and in primary MLECs isolated from NOX1-deficient mice (Figures 4C and 4D). These results indicate that NOX1 but not NOX2 is mainly responsible for ROS formation in lungs and in primary type II AECs and MLECs.

NOX1 Deficiency But Not NOX2 Prevents Cell Death in Lungs and in Primary Alveolar Cells

Because ROS contribute to oxidant-induced cell death in several animal models and in humans, we investigated whether NOX1 and NOX2 participate in alveolar cell death during hyperoxia through ROS generation. First, we examined in situ DNA strand breaks by fluorescence TUNEL staining. Hyperoxia increased significantly the number of TUNEL-positive cells in the lungs of WT mice and NOX2-deficient mice. By contrast, a much lower number of cells was positive when derived from NOX1-deficient mice under hyperoxia (Figures 5A and 5B). These results were supported by those obtained with primary type II AECs and MLECs isolated from hyperoxia-exposed WT mice and from NOX2- and NOX1-deficient mice (Figures 5C and 5D).

Zhang and colleagues reported that caspase-3 activation participated in oxidant-induced DNA fragmentation and cell death in MLE-12 cells (6). We therefore examined whether ROS-induced cell death in situ involved caspase-3 activation and subsequent PARP-1 cleavage. In hyperoxic lungs, there was a significant increase in the amount of cleaved caspase-3 (17 kD) and cleaved PARP-1 (85 kD) in WT mice, whereas in NOX1-deficient mice only small increases were observed (Figures 6A–6C). Indeed, the cleavage of procaspase-3 (32 kD) resulted in two fragments: a 19-kD fragment and a 17-kD fragment, with the 17-kD fragment being the active form of
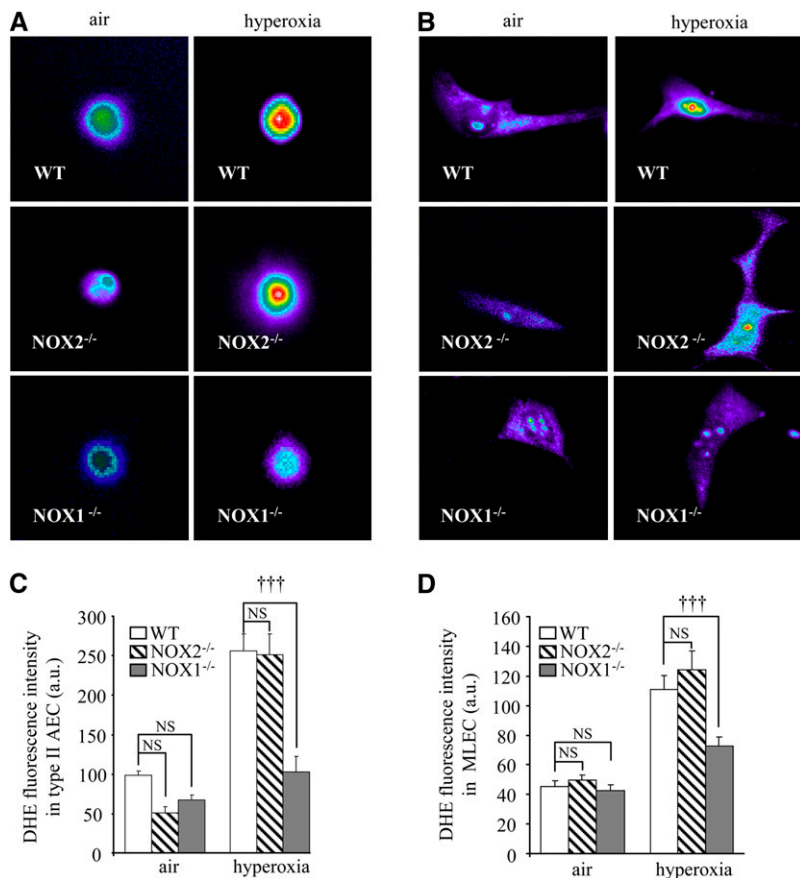
Figure 4. Absence of NADPH oxidase-1 (NOX1) decreased reactive oxygen species generation induced by hyperoxia in primary pulmonary type II alveolar epithelial cells (AECs) and in mouse lung endothelial cells (MLECs). (*A*) Isolated type II AECs and (*B*) MLECs from NOX1$^{-/-}$, NOX2$^{-/-}$, and wild-type (WT) mice were exposed to hyperoxia for 24 hours and loaded with dihydroethidium (DHE, 5 μM) and visualized by confocal microscopy (*pseudocolor*). Original magnification, ×100. (*C* and *D*) Quantification of DHE fluorescence intensity of type II AECs and MLECs. Values represent means and SEM (n = 3 mice for each group; $^{†††}P < 0.001$, NOX1$^{-/-}$ vs. WT mice in hyperoxia; and P = not significant [NS], NOX2$^{-/-}$ vs. WT mice in hyperoxia).
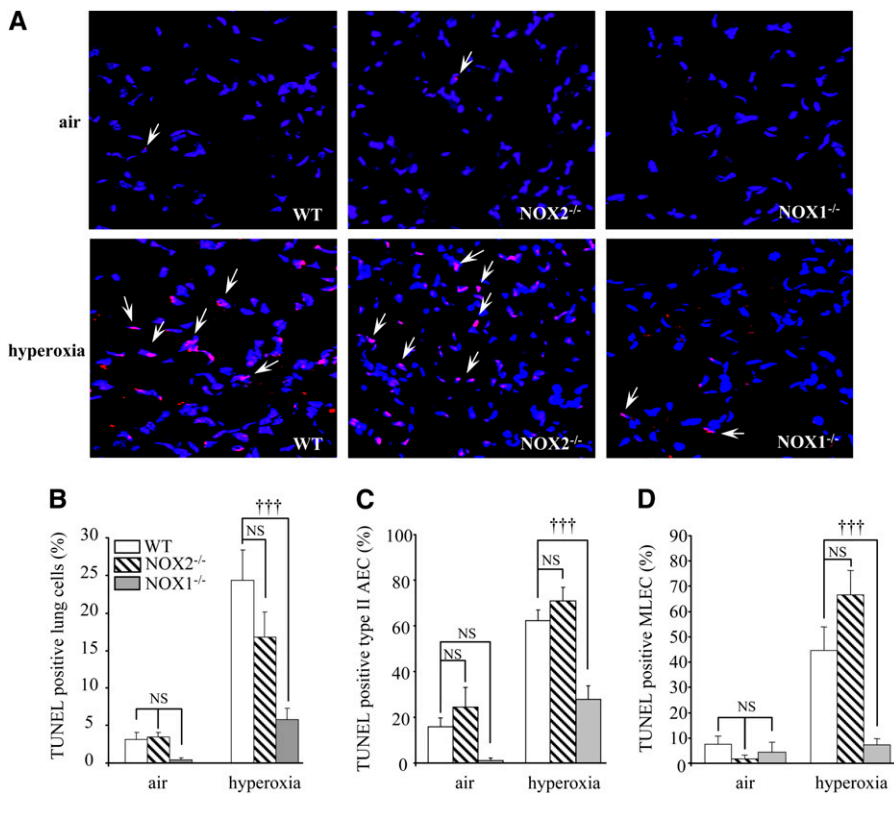
Figure 5. Cell death is decreased in lung cells of NADPH oxidase-1 (NOX1)-deficient mice but not in those of NADPH oxidase-2 (NOX2)-deficient mice. (*A*) Representative merged images of lung sections stained with terminal deoxynucleotidyltransferase–mediated dUTP nick end labeling (TUNEL) stain (*red*) and with 4′,6-diamidino-2-phenylindole (*blue*) from NOX1$^{-/-}$, NOX2$^{-/-}$, and wild-type (WT) mouse lungs. Original magnification, ×40. *Arrows* indicate representative TUNEL-positive cells, which appear *pink*. (*B*) Quantification of TUNEL-positive cells was performed by counting the number of TUNEL-positive cells (appearing *pink*) related to the total number of nuclei (appearing *blue*). *Columns* and *error bars* represent means and SEM (10 fields/mouse, n = 3 mice for each group; $^{†††}P < 0.001$, NOX1$^{-/-}$ vs. WT mouse lung sections; P = NS, NOX2$^{-/-}$ vs. WT mouse lung sections in hyperoxia). (*C* and *D*) Primary type II alveolar epithelial cells (AECs) and mouse lung endothelial cells (MLECs) isolated from NOX1$^{-/-}$, NOX2$^{-/-}$, and WT mice were exposed to air or hyperoxia for 72 hours. Quantification of TUNEL-positive cells was performed by counting the number of TUNEL-positive AECs and MLECs relative to the total number of nuclei. *Columns* and *error bars* represent means and SEM (isolation of three different mice for each group; $^{†††}P < 0.001$, NOX1$^{-/-}$ vs. WT hyperoxia-exposed cells; and P = NS, NOX2$^{-/-}$ vs. WT hyperoxia-exposed cells).

caspase-3 responsible for PARP-1 cleavage (31). We confirmed these results on lung sections from air- and hyperoxia-exposed WT and NOX1-deficient mice, using cleaved caspase-3 immunofluorescence staining (Figure 6D). In hyperoxia, there was a fivefold increase in caspase-3–positive cells compared with air in WT mice, whereas only a few positive cells were found in NOX1-deficient lungs: 5.6 ± 0.7% for WT mice versus 1.1 ± 0.2% for NOX1-deficient mice (the values are expressed as the mean percentage ± SEM; $P < 0.001$, n = 3). These data

demonstrate that under hyperoxic conditions, NOX1-generated ROS but not NOX2-generated ROS mediate lung cell death, and NOX1 modulates the caspase-3–dependent apoptotic process.

ROS Generated by NOX1 Mediate JNK and ERK Phosphorylation in Mouse Lungs during Hyperoxia

To determine the mechanisms by which NOX1-derived ROS are responsible for lung alveolar cell death, we examined ROS-
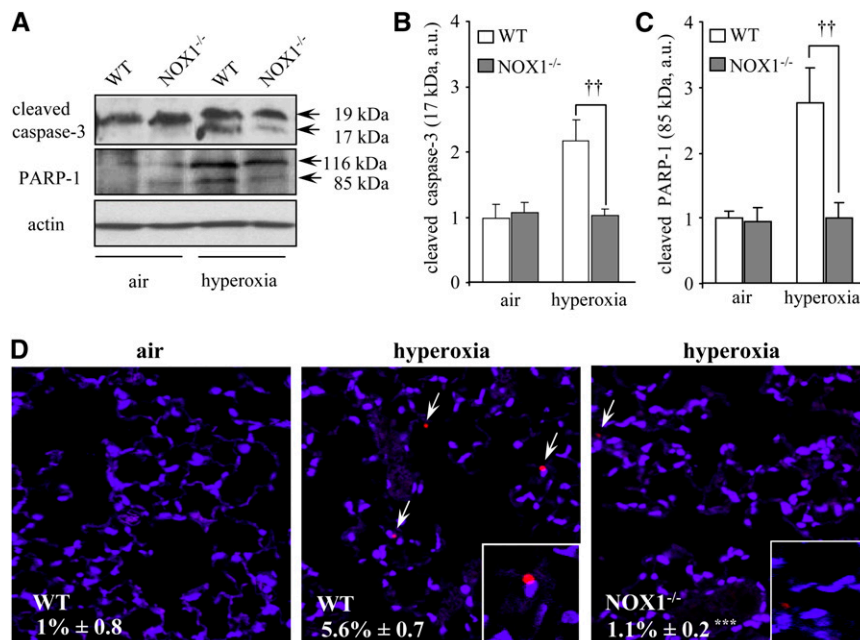
Figure 6. Active caspase-3 and poly(ADP-ribose) polymerase (PARP)-1 cleavage are reduced in the lungs of hyperoxia-exposed NADPH oxidase-1 (NOX1)-deficient mice. (*A*) Cleaved caspase-3 (17 kD) and cleaved PARP-1 (85 kD) proteins were detected in lung homogenates of NOX1$^{-/-}$ and wild-type (WT) mice exposed to air or hyperoxia for 72 hours. β-Actin–immunoreactive bands were used to demonstrate equal loading. These gels were representative of all samples analyzed (n = 5 per group). (*B* and *C*) Densitometric quantification of cleaved caspase-3 and cleaved PARP-1 protein levels was expressed as fold increase compared with WT air sample (set as 1). Each sample was normalized with β-actin loading. *Columns* and *error bars* represent means and SEM (n = 5; $^{††}P < 0.01$, NOX1$^{-/-}$ vs. WT mice in hyperoxia). (*D*) Representative merged images of lung sections stained with anti–cleaved caspase-3 (*red*) and 4′,6-diamidino-2-phenylindole (*blue*) from WT and NOX1$^{-/-}$ mice (n = 3). Original magnification, ×40. $^{***}P < 0.001$, NOX1$^{-/-}$ vs. WT mice in hyperoxia.

involved MAPK (JNK and ERK) pathways. Hyperoxia was associated with a significant increase in pJNKs and pERKs in WT mice as seen by Western blot. NOX1, but not NOX2, deficiency decreased ERK and JNK phosphorylation without modification of JNK and ERK protein levels (Figures 7A–7F).

To identify cell types involved in ERK and JNK activation in hyperoxia, lung sections from WT and NOX1-deficient mice were immunostained with an anti-pERK or pJNK antibody combined with an anti–SP-C antibody or an anti-VWF antibody. pERK staining was associated with type II pneumocytes and endothelial cell markers during hyperoxia (Figure 8A), whereas pJNK staining was detected mainly in endothelial cells (Figure 8B). The staining for pERKs and pJNKs was attenuated in lungs from NOX1-deficient mice (Figure 8A, panels b and c and panels e and f, respectively; and Figure 8B, panels b and c and panels e and f, respectively), confirming the results obtained by Western blotting (Figures 7D−7F). Some cells were positive for pJNK in hyperoxia that were neither SP-C– nor VWF-positive cells. Therefore, according to their localization and the absence of staining, we concluded that these cells were most probably alveolar macrophages (Figure 8B, panels c–f). These data demonstrate that NOX1 participates in oxidative stress–induced acute lung injury, involving ERK and JNK phosphorylation of pulmonary endothelial and epithelial type II cells.

DISCUSSION

NOX enzymes are considered critical contributors to a variety of diseases including cancers, cardiovascular disease, and diabetes. NOX1 has been shown to be expressed in a large number of tissues, including the lung, but its precise function has not been determined yet (20, 32). Several studies have demonstrated a role for NOX1 in the vascular system: NOX1 deficiency decreased blood pressure and provided protection from aortic dissection and aneurysm formation in response to angiotensin II (17, 18, 33).

In the present study, we found that NOX1, but not NOX2, participates in hyperoxia-induced lung injury through decreased ROS generation and cell death in alveolar epithelial and endothelial cells. Cell death prevention was associated with decreased phosphorylation of two main components of MAPK pathways: pERK and pJNK, two enzymes involved in the cell death pathway. In NOX1- and NOX2-deficient mice, exposure to hyperoxia leads to a huge neutrophil influx in BAL fluid, higher than in WT mice. Our results are supported by previous studies (34). Indeed, NOX2-deficient mice exposed to 48 hours of hyperoxia after acid aspiration, and p47^{phox}- or NOX2-deficient mice infected with *Escherichia coli*, showed a greater amount of neutrophils compared with WT mice, without modification of lung injury (35). Moreover, a similar increased lung inflammatory response was noticed after influenza virus infection in NOX2-deficient mice, but in this case it was associated with reduced lung damage and improved lung function (36). Our data are also consistent with previous studies showing that neutrophil or macrophage depletion did not change lung damage in hyperoxic lung injury (37, 38). Indeed, hyperoxia-induced acute lung injury is one of the most established models of oxidative stress and alveolar cell death, which is not closely linked to the magnitude of the inflammatory response; in this way it is different from most cases of human acute respiratory distress syndrome (39). However, in another study, hyperoxia-exposed NOX2-deficient mice produced a lower number of neutrophils in BAL fluid compared with WT mice (22). In that study, mice exposed to acute hyperoxia developed lung fibrosis that was accompanied by a large inflammatory response. Because fibrosis is not a classical pattern of acute hyperoxic lesions,
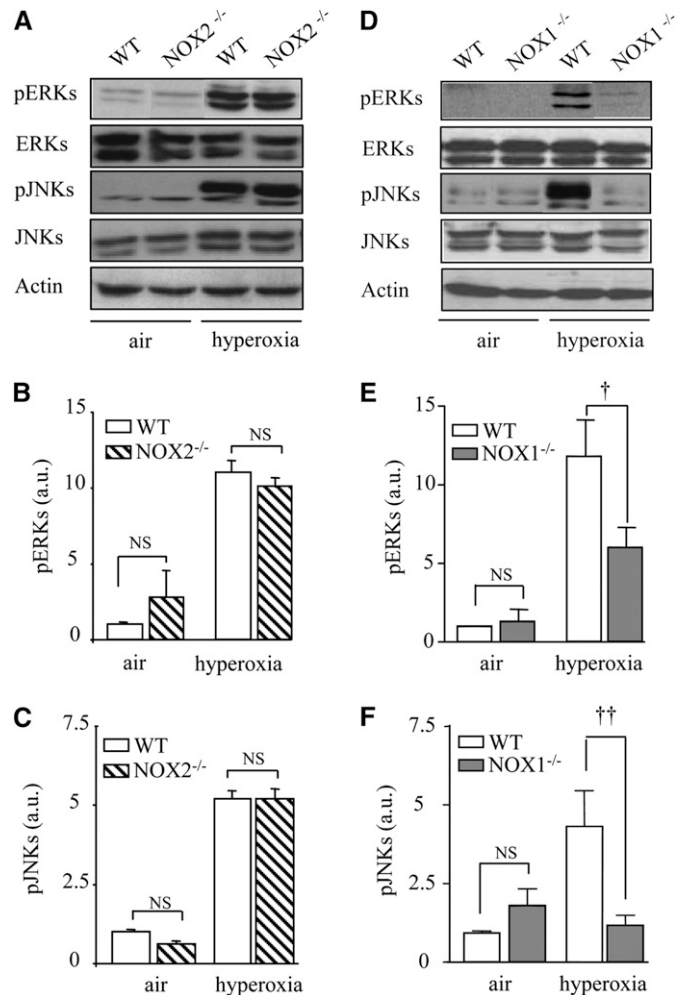
Figure 7. NADPH oxidase-1 (NOX1) mediates the phosphorylation of extracellular signal–regulated kinases (ERKs) and c-Jun N-terminal kinases (JNKs). (*A* and *D*) Western blots for phosphorylated ERKs (pERKs), phosphorylated JNKs (pJNKs), and total ERKs and JNKs. Lung lysates (50 μg) from NOX1$^{-/-}$, NOX2$^{-/-}$, or wild-type (WT) mice were loaded. β-Actin–immunoreactive bands were used to demonstrate equal loading. Theses gels were representative of all samples analyzed (n = 5 per group). (*B*, *C*, *E*, and *F*) Densitometric quantifications of pERKs and pJNKs were determined by comparing experimental sample with WT air sample. Each sample was normalized for β-actin loading. *Columns* and *error bars* represent means and SEM (n = 5 mice; $^{††}P < 0.01$, NOX1$^{-/-}$ vs. WT mice in hyperoxia; $^{†}P < 0.05$, NOX1$^{-/-}$ vs. WT mice in hyperoxia; and $P = NS$, NOX2$^{-/-}$ vs. WT mice in hyperoxia).

we cannot compare our data with these results. Our study suggests that protection provided by NOX1 deficiency during hyperoxia is not due to decreased ROS production by lung inflammatory cells, where NOX2 is preferentially expressed.

The results of this study demonstrate that hyperoxia-induced oxidative stress and tissue damage is, at least in part, mediated by NOX1. One of the reasons for the important role of NOX1 in hyperoxia might lie in the spatial localization of NOX1 in the lung. Primary pulmonary epithelial type II and lung endothelial cells expressed NOX1. Therefore, NOX1 is strategically located to be exposed to high oxygen concentration and to cause damage to the alveolocapillary barrier. A biochemical feature that distinguishes NOX1 from NOX2 might also play an important role. NOXO1, the organizer subunit of the NOX1 enzyme complex, lacks an autoinhibitory domain (40) and a basal NOX1
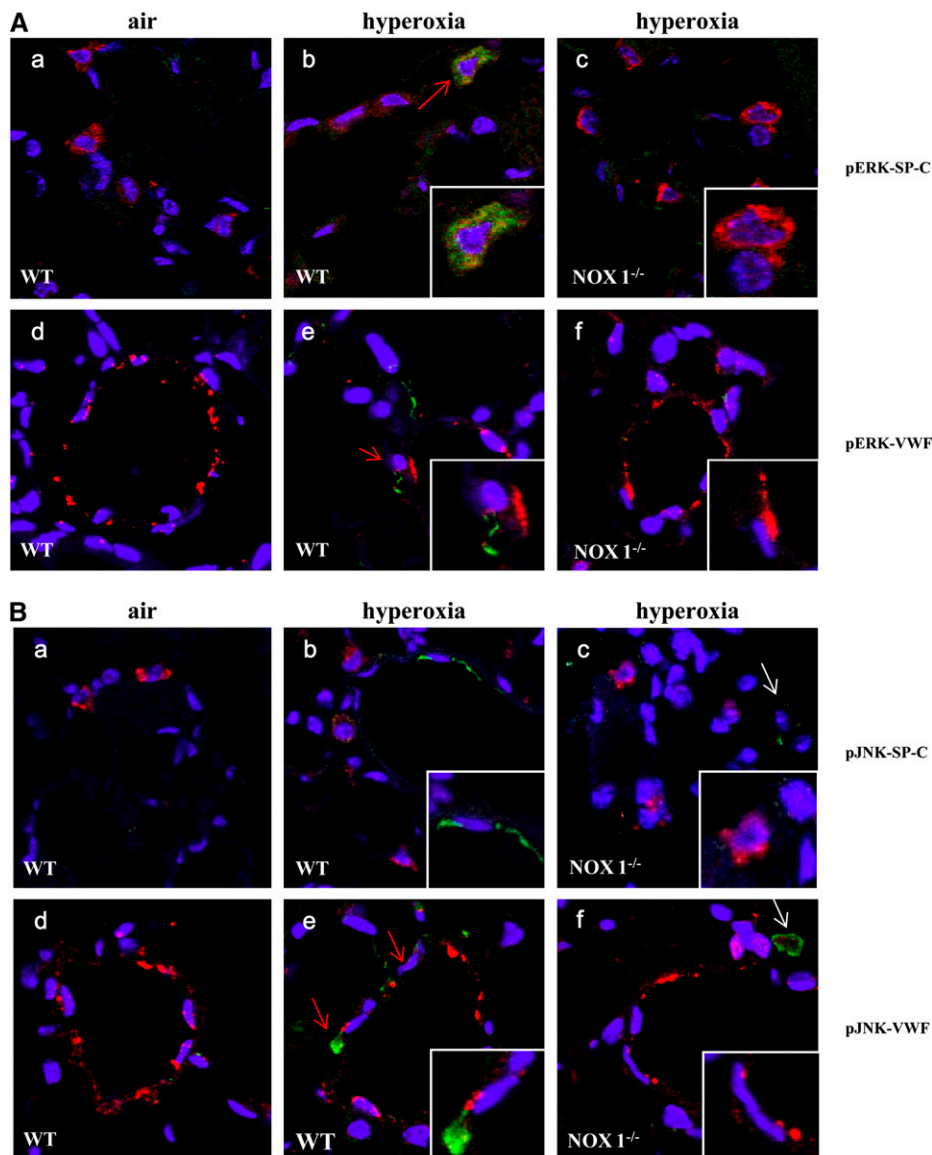
Figure 8. NADPH oxidase-1 (NOX1) mediates the phosphorylation of extracellular signal–regulated kinases (pERKs) and c-Jun N-terminal kinases (pJNKs) in alveolar type II epithelial cells and in endothelial cells. (*A*) Representative merged images of lung sections stained with anti-pERKs (*green*), 4′,6-diamidino-2-phenylindole (DAPI, *blue*), and anti–prosurfactant protein-C (SP-C, *red*; panels a–c) or anti–von Willebrand factor (VWF, *red*; panels d–f) (original magnification, ×63). Note that pERK staining was colocalized with the marker for type II epithelial cells and endothelial cells (*red arrows*, panels b and e). (*B*) Representative merged images of lung sections stained with anti-pJNK (*green*), DAPI (*blue*), and anti–SP-C (*red*, panels a–c) or anti-VWF (*red*; panels d–f) (original magnification, ×63). Note that pJNK staining is not exclusively restricted to endothelial cells but is also present in macrophages (*white arrows*). pJNK and pERK cytoplasmic staining is attenuated in NOX1$^{-/-}$ lungs compared with wild-type (WT) lungs.

activity level has therefore been consistently reported (11). Thus, in contrast to NOX2, which is basically inactive in the absence of cell activation, we found that NOX1 is able to directly increase its ROS generation in response to the elevation of its substrate oxygen in murine alveolar epithelial type II and endothelial cells. In addition to increased substrate, that is, oxygen concentration, other mechanisms might contribute to the increased NOX1 activation under hyperoxic conditions, for example, kinase activation and/or activation of Rac GTPases (41).

NOX1 expression was increased in both epithelial and endothelial cells during hyperoxia. Specific absence of NOX1 decreased hyperoxia-induced ROS generation within the lung and specifically in pulmonary epithelial and endothelial cells. Decreased ROS production was significantly associated with less alveolar cell death as shown by DNA fragmentation markers, such as TUNEL staining and decreased active caspase-3 (17 kD) and PARP-1 cleavage. Also, DPI treatment, a nonspecific inhibitor of NOX enzymes and other electron transporters, decreased hyperoxia-induced ROS generation in human artery endothelial cells and oxidant-induced cell death in MLE-12 cells (6, 9). This cell death reduction was associated

with decreased caspase-3 activation and PARP-1 cleavage in MLE-12 cells (6).

In the present study, hyperoxia activated both pERK and pJNK in mouse lungs as already reported (42) and particularly in pulmonary type II epithelial and endothelial cells. Interestingly, pJNK was found mostly in lung endothelial cells during hyperoxia, suggesting differential MAPK activation *in vivo*. The absence of NOX1 but not NOX2 decreased hyperoxia-induced JNK and ERK phosphorylation in alveolar cells. In accordance with these observations, treatment with DPI completely inhibited hyperoxia-induced ERK1/2 activation and subsequent cell death in alveolar epithelial cells (6, 43). Furthermore, the response to tumor necrosis factor–induced JNK activity and cell death was inhibited in alveolar epithelial cells transfected with NOX1-specific small interfering RNA (44, 45). It is interesting to note that JNK activation was similarly detectable in alveolar macrophages during hyperoxia in NOX1-deficient mice and in WT mice, thus attesting to the specificity of JNK activation by NOX1 in alveolar cells (46). The precise redox-sensible step involved in kinase activation in response to NOX-dependent ROS production is presently unknown. It may be due to inhibition of MAPK tyrosine phosphatase activity or activation of

apoptosis signal-regulating kinase-1 (ASK1)-dependent or -independent pathways (44, 47, 48). It has been proposed that ROS, via the oxidation of thioredoxin, a redox regulatory protein, leads to ASK1 liberation and to tumor necrosis factor–induced JNK activation in MLE-12 cells (44). We also explored Akt phosphorylation (pAkt), because the instillation of the constitutively active form of Akt in mice before exposure to hyperoxia protected lung from oxidant-induced lung damage (49). Our results did not favor the hypothesis that a change in pAkt could mediate lung cell protection in NOX1-deficient mice (data not shown), but they strongly suggest that ROS generated by NOX1 participate specifically in the signaling of hyperoxia-induced ERK and JNK activation and thereby induce alveolar cell death in mouse lung.

Our data are the first direct demonstration that NOX1 activation promotes apoptosis *in vivo* and especially in the cells that comprise the alveolocapillary barrier. The results are not compatible with the hypothesis that ROS released by mitochondria are the *primum movens* of hyperoxic oxidative stress. We also found that NOX-derived ROS cause DNA strand breaks *in vivo*. However, it is not clear at this point whether NOX1-derived ROS are responsible for direct genotoxic stress or whether the DNA strand breaks are also due to caspase activation by redox-sensitive cell death pathways (e.g., JNK and ERK). Indeed, it is likely that caspase activation is not sufficient to fully account for the DNA strand breaks observed in response to hyperoxia because (*1*) in this study, we observed a smaller number of caspase-3–positive cells, as compared with TUNEL-positive cells; and (*2*) in previous studies we found that administration of pan-caspase inhibitor (Z-VAD) was not sufficient to rescue hyperoxia-induced cell death (3, 50). If direct genotoxic stress through NOX1-derived ROS is a contributor to hyperoxic lung damage, it is essential to inhibit ROS formation at a significantly upstream level. This approach could have an important impact on future therapeutic developments, potentially favoring the targeting of NOX1-specific inhibitors over inhibition of redox-sensitive cell death pathways in the treatment of acute lung injury.

References

1. Tasaka S, Amaya F, Hashimoto S, Ishizaka A. Roles of oxidants and redox signaling in the pathogenesis of acute respiratory distress syndrome. *Antioxid Redox Signal* 2008;10:739–753.
2. Roper JM, Mazzatti DJ, Watkins RH, Maniscalco WM, Keng PC, O'Reilly MA. *In vivo* exposure to hyperoxia induces DNA damage in a population of alveolar type II epithelial cells. *Am J Physiol Lung Cell Mol Physiol* 2004;286:L1045–L1054.
3. Barazzone C, Horowitz S, Donati YR, Rodriguez I, Piguet PF. Oxygen toxicity in mouse lung: pathways to cell death. *Am J Respir Cell Mol Biol* 1998;19:573–581.
4. Zaher TE, Miller EJ, Morrow DM, Javdan M, Mantell LL. Hyperoxia-induced signal transduction pathways in pulmonary epithelial cells. *Free Radic Biol Med* 2007;42:897–908.
5. Lee PJ, Choi AM. Pathways of cell signaling in hyperoxia. *Free Radic Biol Med* 2003;35:341–350.
6. Zhang X, Shan P, Sasidhar M, Chupp GL, Flavell RA, Choi AM, Lee PJ. Reactive oxygen species and extracellular signal–regulated kinase 1/2 mitogen-activated protein kinase mediate hyperoxia-induced cell death in lung epithelium. *Am J Respir Cell Mol Biol* 2003;28:305–315.
7. Romashko J III, Horowitz S, Franek WR, Palaia T, Miller EJ, Lin A, Birrer MJ, Scott W, Mantell LL. MAPK pathways mediate hyper-oxia-induced oncotic cell death in lung epithelial cells. *Free Radic Biol Med* 2003;35:978–993.
8. Li Y, Arita Y, Koo HC, Davis JM, Kazzaz JA. Inhibition of c-Jun N-terminal kinase pathway improves cell viability in response to oxidant injury. *Am J Respir Cell Mol Biol* 2003;29:779–783.
9. Parinandi NL, Kleinberg MA, Usatyuk PV, Cummings RJ, Pennathur A, Cardounel AJ, Zweier JL, Garcia JG, Natarajan V. Hyperoxia-induced NAD(P)H oxidase activation and regulation by MAP kinases in human lung endothelial cells. *Am J Physiol Lung Cell Mol Physiol* 2003;284:L26–L38.
10. Li J, Gao X, Qian M, Eaton JW. Mitochondrial metabolism underlies hyperoxic cell damage. *Free Radic Biol Med* 2004;36:1460–1470.
11. Lambeth JD. NOX enzymes and the biology of reactive oxygen. *Nat Rev Immunol* 2004;4:181–189.
12. Bedard K, Krause KH. The NOX family of ROS-generating NADPH oxidases: physiology and pathophysiology. *Physiol Rev* 2007;87:245–313.
13. Babior BM. The leukocyte NADPH oxidase. *Isr Med Assoc J* 2002;4:1023–1024.
14. Carnesecchi S, Carpentier JL, Foti M, Szanto I. Insulin-induced vascular endothelial growth factor expression is mediated by the NADPH oxidase NOX3. *Exp Cell Res* 2006;312:3413–3424.
15. Ameziane-El-Hassani R, Morand S, Boucher JL, Frapart YM, Apostolou D, Agnandji D, Gnidehou S, Ohayon R, Noel-Hudson MS, Francon J, *et al.* Dual oxidase-2 has an intrinsic Ca^{2+}-dependent H_2O_2-generating activity. *J Biol Chem* 2005;280:30046–30054.
16. Wu DC, Re DB, Nagai M, Ischiropoulos H, Przedborski S. The inflammatory NADPH oxidase enzyme modulates motor neuron degeneration in amyotrophic lateral sclerosis mice. *Proc Natl Acad Sci USA* 2006;103:12132–12137.
17. Gavazzi G, Banfi B, Deffert C, Fiette L, Schappi M, Herrmann F, Krause KH. Decreased blood pressure in NOX1-deficient mice. *FEBS Lett* 2006;580:497–504.
18. Gavazzi G, Deffert C, Trocme C, Schappi M, Herrmann FR, Krause KH. NOX1 deficiency protects from aortic dissection in response to angiotensin II. *Hypertension* 2007;50:189–196.
19. Zhang X, Shan P, Jiang G, Cohn L, Lee PJ. Toll-like receptor 4 deficiency causes pulmonary emphysema. *J Clin Invest* 2006;116:3050–3059.
20. Mittal M, Roth M, Konig P, Hofmann S, Dony E, Goyal P, Selbitz AC, Schermuly RT, Ghofrani HA, Kwapiszewska G, *et al.* Hypoxia-dependent regulation of nonphagocytic NADPH oxidase subunit NOX4 in the pulmonary vasculature. *Circ Res* 2007;101:258–267.
21. Goyal P, Weissmann N, Grimminger F, Hegel C, Bader L, Rose F, Fink L, Ghofrani HA, Schermuly RT, Schmidt HH, *et al.* Upregulation of NAD(P)H oxidase 1 in hypoxia activates hypoxia-inducible factor 1 via increase in reactive oxygen species. *Free Radic Biol Med* 2004;36:1279–1288.
22. Natarajan V, Pendyala S, Gorshkova IA, Usatyuk P, He D, Pennathur A, Lambeth JD, Thannickal VJ. Role of Nox4 and Nox2 in hyperoxia-induced reactive oxygen species generation and migration of human lung endothelial cells. *Antioxid Redox Signal* 2009;11:747–764.
23. Carnesecchi S, Deffert C, Pagano A, Metrailler-Ruchonnet I, Donati Y, Matthay M, Krause KH, Barazzone-Argiroffo C. NADPH oxidase (NOX1) is essential in hyperoxia-induced lung damage [abstract]. *Am J Respir Crit Care Med* 2009;179:A5364.
24. Pollock JD, Williams DA, Gifford MA, Li LL, Du X, Fisherman J, Orkin SH, Doerschuk CM, Dinauer MC. Mouse model of X-linked chronic granulomatous disease, an inherited defect in phagocyte superoxide production. *Nat Genet* 1995;9:202–209.
25. Barazzone C, Belin D, Piguet PF, Vassalli JD, Sappino AP. Plasminogen activator inhibitor-1 in acute hyperoxic mouse lung injury. *J Clin Invest* 1996;98:2666–2673.
26. Zhou H, Imrich A, Kobzik L. Characterization of immortalized MARCO and SR-AI/II–deficient murine alveolar macrophage cell lines. *Part Fibre Toxicol* 2008;5:7.
27. Reynolds LE, Hodivala-Dilke KM. Primary mouse endothelial cell culture for assays of angiogenesis. *Methods Mol Med* 2006;120:503–509.
28. Corti M, Brody AR, Harrison JH. Isolation and primary culture of murine alveolar type II cells. *Am J Respir Cell Mol Biol* 1996;14:309–315.
29. Pagano A, Donati Y, Metrailler I, Barazzone Argiroffo C. Mitochondrial cytochrome *c* release is a key event in hyperoxia-induced lung injury: protection by cyclosporin A. *Am J Physiol Lung Cell Mol Physiol* 2004;286:L275–L283.

30. Chu SJ, Perng WC, Hung CM, Chang DM, Lin SH, Huang KL. Effects of various body temperatures after lipopolysaccharide-induced lung injury in rats. *Chest* 2005;128:327–336.

31. Zhan Y, van de Water B, Wang Y, Stevens JL. The roles of caspase-3 and bcl-2 in chemically-induced apoptosis but not necrosis of renal epithelial cells. *Oncogene* 1999;18:6505–6512.

32. Cheng G, Cao Z, Xu X, van Meir EG, Lambeth JD. Homologs of gp91phox: cloning and tissue expression of Nox3, Nox4, and Nox5. *Gene* 2001;269:131–140.

33. Matsuno K, Yamada H, Iwata K, Jin D, Katsuyama M, Matsuki M, Takai S, Yamanishi K, Miyazaki M, Matsubara H, *et al.* Nox1 is involved in angiotensin II-mediated hypertension: a study in Nox1-deficient mice. *Circulation* 2005;112:2677–2685.

34. Schappi M, Deffert C, Fiette L, Gavazzi G, Herrmann F, Belli D, Krause KH. Branched fungal β-glucan causes hyperinflammation and necrosis in phagocyte NADPH oxidase-deficient mice. *J Pathol* 2008;214:434–444.

35. Gao XP, Standiford TJ, Rahman A, Newstead M, Holland SM, Dinauer MC, Liu QH, Malik AB. Role of NADPH oxidase in the mechanism of lung neutrophil sequestration and microvessel injury induced by gram-negative sepsis: studies in p47phox$^{-/-}$ and gp91phox$^{-/-}$ mice. *J Immunol* 2002;168:3974–3982.

36. Snelgrove RJ, Edwards L, Rae AJ, Hussell T. An absence of reactive oxygen species improves the resolution of lung influenza infection. *Eur J Immunol* 2006;36:1364–1373.

37. Berg JT, White JE, Tsan MF. Response of alveolar macrophage-depleted rats to hyperoxia. *Exp Lung Res* 1995;21:175–185.

38. Boyce NW, Campbell D, Holdsworth SR. Granulocyte independence of pulmonary oxygen toxicity in the rat. *Exp Lung Res* 1989;15:491–498.

39. Martin TR, Pistorese BP, Chi EY, Goodman RB, Matthay MA. Effects of leukotriene B$_4$ in the human lung: recruitment of neutrophils into the alveolar spaces without a change in protein permeability. *J Clin Invest* 1989;84:1609–1619.

40. Banfi B, Clark RA, Steger K, Krause KH. Two novel proteins activate superoxide generation by the NADPH oxidase NOX1. *J Biol Chem* 2003;278:3510–3513.

41. Werner E, Werb Z. Integrins engage mitochondrial function for signal transduction by a mechanism dependent on Rho GTPases. *J Cell Biol* 2002;158:357–368.

42. Yang G, Abate A, George AG, Weng YH, Dennery PA. Maturational differences in lung NF-κB activation and their role in tolerance to hyperoxia. *J Clin Invest* 2004;114:669–678.

43. Papaiahgari S, Kleeberger SR, Cho HY, Kalvakolanu DV, Reddy SP. NADPH oxidase and ERK signaling regulates hyperoxia-induced Nrf2-ARE transcriptional response in pulmonary epithelial cells. *J Biol Chem* 2004;279:42302–42312.

44. Pantano C, Anathy V, Ranjan P, Heintz NH, Janssen-Heininger YM. Nonphagocytic oxidase 1 causes death in lung epithelial cells via a TNF–RI–JNK signaling axis. *Am J Respir Cell Mol Biol* 2007;36:473–479.

45. Kim YS, Morgan MJ, Choksi S, Liu ZG. TNF-induced activation of the Nox1 NADPH oxidase and its role in the induction of necrotic cell death. *Mol Cell* 2007;26:675–687.

46. Iles KE, Forman HJ. Macrophage signaling and respiratory burst. *Immunol Res* 2002;26:95–105.

47. Chowdhury AK, Watkins T, Parinandi NL, Saatian B, Kleinberg ME, Usatyuk PV, Natarajan V. Src-mediated tyrosine phosphorylation of p47^{phox} in hyperoxia-induced activation of NADPH oxidase and generation of reactive oxygen species in lung endothelial cells. *J Biol Chem* 2005;280:20700–20711.

48. Kamata H, Honda S, Maeda S, Chang L, Hirata H, Karin M. Reactive oxygen species promote TNFα-induced death and sustained JNK activation by inhibiting MAP kinase phosphatases. *Cell* 2005;120:649–661.

49. Lu Y, Parkyn L, Otterbein LE, Kureishi Y, Walsh K, Ray A, Ray P. Activated Akt protects the lung from oxidant-induced injury and delays death of mice. *J Exp Med* 2001;193:545–549.

50. Metrailler-Ruchonnet I, Pagano A, Carnesecchi S, Ody C, Donati Y, Barazzone Argiroffo C. Bcl-2 protects against hyperoxia-induced apoptosis through inhibition of the mitochondria-dependent pathway. *Free Radic Biol Med* 2007;42:1062–1074.